Isolated-core excitations in strong electric fields. II. Experimental results in magnesium

J. B. M. Warntjes,[1] F. Robicheaux,[1,2] and L. D. Noordam[1]
[1]*FOM-Institute for Atomic and Molecular Physics (AMOLF), Kruislaan 407, 1098-SJ Amsterdam, The Netherlands*
[2]*Department of Physics, Auburn University, Auburn, Alabama 36849*
(Received 14 January 2000; published 17 August 2000)

We report on the electron yield spectra of doubly excited magnesium atoms in electric fields in the region 50–1600 V/cm. One electron is excited to a stationary Rydberg state around $n=16$, either a nonmixing state with low angular momentum or a Stark state. Subsequently the second isolated-core electron is excited with a narrow-band nanosecond laser pulse. The isolated-core excitation induces a shake-up which is measured as a function of excitation frequency. An initial low-angular-momentum state leads to a much broader shakeup than an initial Stark state, i.e., many more autoionization peaks are observed for an initial low-angular-momentum state than for an initial Stark state. Full quantum calculations introduced in the preceding paper [F. Robicheaux, preceding paper Phys. Rev. A **61**, 033406 (2000)] show excellent agreement with the recorded spectra. We discuss the implications of this experiment for dielectronic recombination and compare the frequency spectra to previously reported time-dependent measurements on magnesium [J.B.M. Warntjes *et al.*, Phys. Rev. Lett. **83**, 512 (1999)].

PACS number(s): 32.60.+i, 32.80.Dz, 32.80.Rm

I. INTRODUCTION

Isolated-core excitation (ICE) of two-electron atoms is an established method to create autoionizing Rydberg states where the core electron is used to provide the exit energy to the Rydberg electron [1,2]. Experiments are reported for ICE on magnesium [3–7] and other two-electron atoms [8–10]. In a two-electron system one electron is optically excited to a high Rydberg state. Such an electron can be viewed as a spectator, because of its large spatial extend and, consequently, small electron density in the vicinity of the ionic core. A second laser pulse excites the remaining, isolated, core electron. If the two excited electrons collide, energy exchange can take place causing one electron to decay back to its ground state whereas the other has now gained enough energy to escape the ionic core. When the isolated core electron is not excited by a laser frequency on a resonance of the ion, the spectating Rydberg electron can sometimes absorb or donate the energy difference. The population of off-resonant Rydberg states is called shakeup.

In most cases ICE was studied in field-free conditions. If a static electric field is applied, the core electron state is unlikely to be affected, owing to its small spatial size. The highly excited Rydberg state, on the other hand, will split up into Stark states. Consequently, the shakeup upon ICE in a field will attain completely different states as compared with zero field. Also, the shakeup width may be changed: A Stark state is a mixture of all angular momenta, resulting in an even smaller electron density in the vicinity of the ionic core. One expects that the interaction between the two electrons decreases as compared to zero field. Consequently the shake-up width upon ICE for a Stark state is expected to be smaller than for a low-angular-momentum state.

Following the development of a theoretical approach in the preceding paper [11], we perform a rigorous check with experimental data on magnesium. The initial and final states are populated as a function of excitation frequency with narrow-band nanosecond laser pulses to determine the shakeup in various electric-field strengths and starting from various states. To our knowledge this is the first match between experiment and theory of ICE spectra in a strong electric field, as will be shown in Secs. IV and V.

One of the motivations to study the autoionization in a two-electron system is the relation with its time inverse process, dielectronic recombination (DR) [15–18]. DR is the process in which a free electron collides with an ion and is converted to a doubly excited atom. If one of the two excited electrons decays by sending out a photon, the initially free electron is recombined. Dielectronic recombination is playing a role in astrophysical plasmas. In such plasmas an electric field can generally not be neglected [15]. A spectating ion already exerts a field of 1400 V/cm on another ion at a distance of 100 nm. Measurements of DR are cumbersome and detecting DR as a function of field is a true experimental challenge. With relative ease the autoionization of a two-electron atom is studied. In Sec. VI we dwell upon the information for DR retrieved from ICE autoionization experiments. We find that the total autoionization cross section is identical to the DR cross section. An autoionization measurement allows us to study the partial cross sections with high resolution; we detect the autoionization yield for each principle quantum number n instead over an integrated number of n's, and we find via which final states they decay.

Finally in Sec. VII we compare the Fourier transform of the frequency spectra with reported time-resolved electron emission of magnesium, using the atomic streak camera [7]. The comparison shows the differences of the recurrence of electron density back to the core and the fraction of that density that is emitted on the picosecond time scale.

II. ICE IN MAGNESIUM

In Fig. 1 the laser excitation scheme of the magnesium ICE experiment in an electric field is depicted. The initial

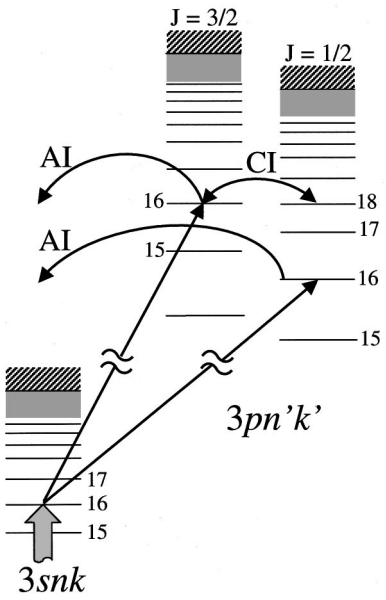

FIG. 1. Excitation scheme for isolated core excitation in magnesium in an electric field. One electron is optically excited to an initial $3snk$, $n=16$ Rydberg state. Subsequently a second laser pulse drives the isolated core electron $3s \rightarrow 3p(\Delta E \sim 4.3$ eV). For clarity only one state is drawn per manifold and the spread of the Stark manifold is not shown. There are two final spin states $p_{1/2}$ and $p_{3/2}$ coupled by configuration interaction (CI). Both the $p_{1/2}$ and $p_{3/2}$ channels are coupled to the $3s$ continuum: Autoionization (AI) occurs when one electron decays to the $3s$ ground state donating its energy to the second electron which escapes the ionic core.

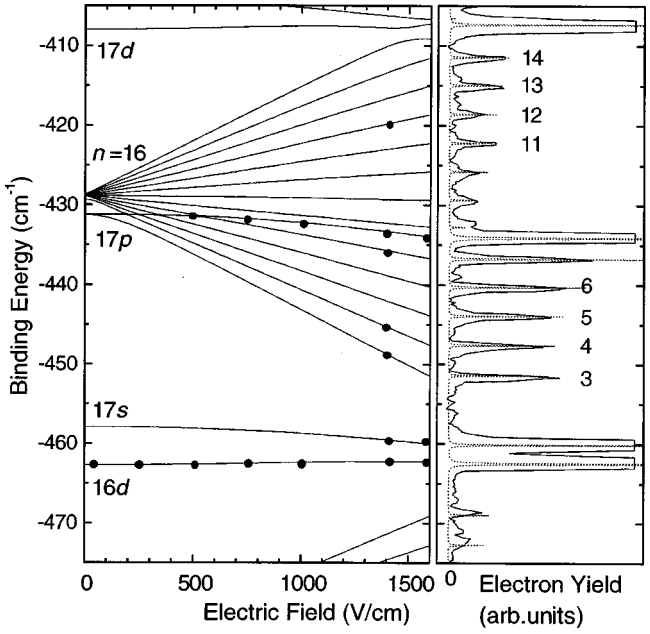

FIG. 2. (a) A calculated Stark map around the Mg $n=16$ manifold in fields up to 1600 V/cm. Dots indicate the experimentally used positions of initial states in the subsequent figures. (b) Experimental 2+1-photon resonant ionization yield spectrum at 1600 V/cm as a function of excitation frequency. The strong peak at the center of the manifold is the $17p$ state, the peaks halfway between manifolds $n=16$ and 15 are the $17s$ and $16d$ states, and the small peaks are the Stark states. The dotted line is the calculation of the two-photon absorption cross section.

Rydberg state is prepared by exciting the $3s^2$ ground state to a Stark state $3snk$ where typically $n=16$. Since the second electron remains in the $3s$ state, we will refer to these initial states $3snk$ as the $3s$ channel. Subsequently the second electron is excited $3s \rightarrow 3p$. There are two final $3pn'k'$ channels, namely the $3p_{1/2}$ and the $3p_{3/2}$ channel, respectively 35 669.42 and 35 760.97 cm^{-1} higher in energy than the $3s$ channel [19]. Upon ICE, the initial $3snk$ state is projected onto the states in the $3p_{1/2}$ or $3p_{3/2}$ channels. Autoionization (AI) then occurs via coupling to the continuum of the $3s$ channel: One electron decays back to the $3s$ ground state donating its energy to the other electron which escapes with ~ 4.3 eV of excess kinetic energy. If the excitation laser is detuned from the $3s \rightarrow 3p$ resonance, the inner electron can still be excited if the Rydberg electron donates or absorbs the energy difference.

Since the two final channels are only separated 91.55 cm^{-1} in energy, their Rydberg series are interleaved and can experience a strong configuration interaction (CI). For example, as one can see from Fig. 1, the $n=16$ manifold of the $3p_{3/2}$ channel is nearly degenerate with the $n=18$ manifold of the $3p_{1/2}$ channel. On the other hand, the $n=16$ of the $3p_{1/2}$ channel has its energy in the middle between the $n=14$ and $n=15$ manifolds of the $3p_{3/2}$ channel. In the latter case configuration interaction could only occur between the extreme red and blue states at the highest field we used, 1600 V/cm. The Δn spacing in this energy region is around 50 cm^{-1}.

III. EXPERIMENTAL SETUP

A resistively heated oven produces an effusive beam of magnesium atoms passing through two parallel metal plates with a static electric field. The distance between the plates is 10.0 mm. The Mg is excited with two narrow-band laser pulses of about 7 ns [full width at half maximum (FWHM)] with a time delay of 20 ns. For the first laser pulse a Nd:YAG (yttrium aluminum gamet) laser pumps a Quantel dye laser producing laser light around 648 nm. The light is frequency doubled with a KDP crystal and drives a two-photon excitation of the Mg ground state to a selected Rydberg Stark state $3s16k$ with a energy of 200 μJ focused down to an intensity of about 10^9 W/cm^2. For the second laser pulse another Nd:YAG laser pumps a Lambda Physics Scanmate dye laser producing laser light around 580 nm. This light is also frequency doubled and drives the one photon $3s$-$3p$ isolated core transition with an intensity of only 10^3 W/cm^2. The bandwidth of both dye lasers is 0.3 cm^{-1} which is sufficient to resolve Stark structure in the used fields. The laser polarization is parallel to the electric field. The autoionized electrons pass through a mesh in one of the metal plates and is detected by a set of microspheroid plates and an anode. The electron emission is monitored as a function of energy of the ICE laser pulse and as a function of field strength between the two metal plates.

IV. RESULTS

We first present the spectroscopy of the initial states $3snk$. Displayed in Fig. 2(a) is a Stark map, calculated in the

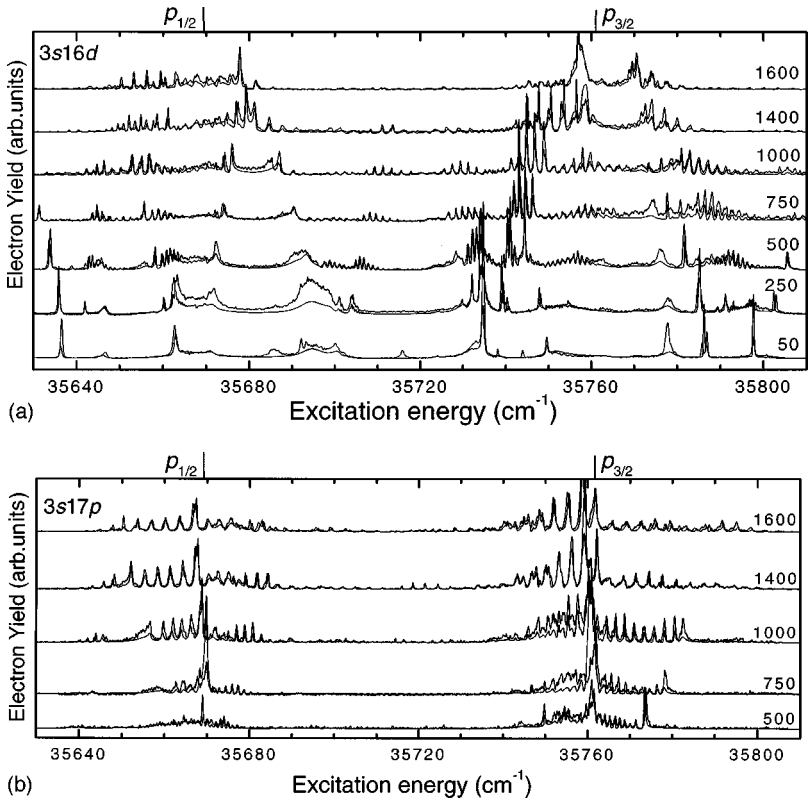

FIG. 3. (a) Electron yield as a function of isolated-core excitation energy starting with the $3s16d$ state in fields of 50 up to 1600 V/cm. The positions of the $3s \rightarrow 3p_{1/2}$ transition at 35 669.42 cm^{-1} and the $3s \rightarrow 3p_{3/2}$ transition at 35 760.97 cm^{-1} are indicated. The smooth lines are the theoretical calculations developed in part I [11]. (b) Same as for (a) with the initial state $3s17p$ in fields of 500 up to 1600 V/cm.

energy range around the $n=16$ manifold in electric fields up to 1600 V/cm. There are a few states with low angular momentum l and a manifold of Stark states that fans out as a function of field. The s and d states have quantum defects δ_l of 1.52 and 0.60, respectively. These states are in the middle between two manifolds and hardly mix with the Stark states in the applied fields. The p state has a quantum defect of 1.05 and is near the center of the Stark manifold. It can, however, only mix with the Stark states if it acquires some d character. Therefore the p state is still quite unaffected by the manifold in fields up to 1600 V/cm. The remaining 13 Stark states fan out approximately linearly as a function of field. We verified the positions of the initial states experimentally. Shown in Fig. 2(b) is the $2+1$ photon resonant ionization yield spectrum as a function of binding energy as detected in a field of 1600 V/cm. Since the photoionization probability is only appreciable for low-l character [20] the $2+1$ photoionization yield spectrum emphasizes the s, p, and d states that are an order of magnitude stronger than the Stark states and off scale in the plot. The dotted line in Fig. 2(b) is the calculated two-photon absorption cross section. The positions of the peaks are accurately reproduced and gives us confidence that, concerning the energy positions of the initial states, the theory matches the experiment. The Stark states are labeled according to their excitation energy from 3 up to 15. The dots in Fig. 2(a) are the selected initial states from where we perform the isolated core excitation.

We first show the results of the initial low-l states which are not much affected by the electric field. For the recorded spectra shown in Fig. 3(a), the $3s16d$ state was selected as initial state. In zero field this state has by far the largest oscillator strength in our two-photon excitation scheme. The autoionization yield after ICE is depicted as a function of excitation frequency of the isolated core electron for various fields. In a field of 50 V/cm, which is nearly field free, we observe a variety of sharp and broad features. The energy range covers a few n states, about $n=16$–18 of the $3p_{1/2}$ channel and $n=15$–16 of the $3p_{3/2}$ channel. Outside this region no signal is observed. As noted by Dai *et al.* [3] the broad features can be attributed to specific $3p_{1/2}nd$ or $3p_{3/2}nd$ $J=3$ states. The sharp peaks are mixtures of $3p_{1/2}nd$ or $3p_{3/2}nd$ $J=1$ states. The shakeup starting from $3s16d$ is so large that the autoionization peaks belonging to both spin channels are interleaved and spread over the whole energy range of Fig. 3(a).

Once the field is increased to 500 V/cm, narrow Stark states appear and the broad features sharpen up. At about 1600 V/cm we only observe Stark states of 1 cm^{-1} width. The spacing between the states is 3.0 cm^{-1} in this field, slightly less than the spacing of the Stark states of the initial $3s$ channel. Note that the laser linewidth is 0.3 cm^{-1}. It is difficult to determine a number for shakeup width from these spectra. To qualitatively get a feeling for the shakeup width we assume that the autoionizing states detected after ICE are in fact two groups of states centered around the $3s \rightarrow 3p_{1/2}$ and the $3s \rightarrow 3p_{3/2}$ transition. The two groups are observed over a certain energy range. Figure 3(a) shows that the shakeup after ICE of an initial d state is rather large; the width is about 100 cm^{-1} at 50 V/cm down to about 50 cm^{-1} in 1600 V/cm for each spin-orbit channel.

In Fig. 3(b) the autoionization yield of an initial $3s17p$ after ICE is depicted as a function of the excitation frequency state for various fields. The initial $3s17p$ state can only be

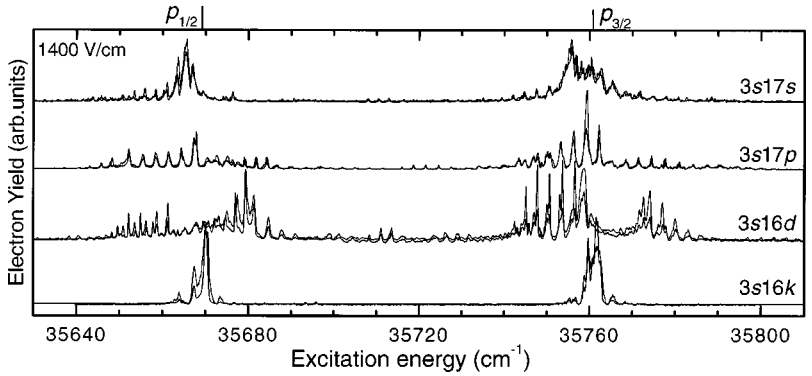

FIG. 4. Electron yield as a function of isolated-core excitation energy starting with the initial state (top to bottom) the 3*s*17*s*, 3*s*17*p*, 3*s*16*d* low-angular-momentum states and the 3 *s*16*k* Stark state with $k=4$ as labeled in Fig. 2(b). The electric field is 1400 V/cm. The energy scale is identical to that used in Fig. 3. The positions of the $3s\rightarrow 3p_{1/2}$ transition at 35 669.42 cm^{-1} and the $3s\rightarrow 3p_{3/2}$ transition at 35 760.97 cm^{-1} are indicated. The smooth lines are the theoretical calculations developed in part I [11].

excited in a field of at least 500 V/cm with a two-photon excitation scheme. The ICE spectrum only consists of sharp Stark states without any broad features. The width of the Stark states is 1 cm^{-1} and the spacing in a field of 1600 V/cm is also 3 cm^{-1}. In all fields the shakeup width is about 50 cm^{-1}. In the ICE spectra of initial low-*l* states in high fields there are no peaks with a large cross section that would indicate a predominant low-*l* character. In the $3p$ channel all states are mixed above 500 V/cm, in striking contrast to the $3s$ channel where we can clearly distinguish the low-*l* states in all fields.

In order to compare the shakeup starting from various initial states, Fig. 4 shows the autoionization yield as a function of excitation frequency of the isolated core electron in a field of 1400 V/cm. The top three curves are spectra taken with $3s17s$, $3s17p$, and $3s16d$ as initial state. All states with low angular momentum in a strong electric field have a shakeup with a width of about 50 cm^{-1}. The richness of the ICE spectrum is dramatically less if we start from a Stark state. The bottom curve in Fig. 4 shows the ICE spectrum starting from an initial $3s16k$ Stark state, with $k=4$. The shakeup only has a width of about 5 cm^{-1}. We have taken spectra at several initial Stark states and observe that all have a similar small shakeup width. In Fig. 5 we show the ICE spectra starting from various initial Stark states and zoom in on the energy axis. In the $P_{1/2}$ channel there is one large peak and, in case of an initial red Stark state ($k=3$-8) a smaller peak on the low-energy side and in case of an initial blue Stark state ($k=10$–15) a smaller peak on the high-energy side. The small and large peak are juxtaposed around the central $3s\rightarrow 3p_{1/2}$ transition at 35 669.42 cm^{-1}. The energy difference between the peaks matches the Stark spacing of 3 cm^{-1}, the width of the peaks is 1 cm^{-1}. In the $P_{3/2}$ channel, on the other hand, we observe more states, up to twice as many as in the $P_{1/2}$ channel depending on the initial Stark state. All peaks are centered around the $3s\rightarrow 3p_{3/2}$ transition at 35 760.97 cm^{-1} also with a shakeup width of 5 cm^{-1}.

The smooth lines in Figs. 3–5 are the MQDT calculations developed in part I [11]. As one can see, the agreement is nearly perfect. To our knowledge this is the first theoretical match on isolated core excitation in a static electric field. Agreement is equally good over the entire range of electric fields and starting from all initial states. We can see in Fig. 3(a) that there is a small deviation between the experimental and theoretical curves at low fields. Saturation effects probably caused the relative increase of broad peaks in the experimental data.

V. DISCUSSION

The energy exchange between the two excited electrons upon ICE can only occur in the core region. In the absence of a field the Rydberg electron spends only a fraction of it radial oscillation time ($\tau_n=2\pi n^3$, 0.6 ps for $n=16$ [21]) in the vicinity of the core and is viewed as a spectator. This restricts the probability of transition to the final $3p$ states to a certain shakeup width. This shakeup width of $n=16$ is about

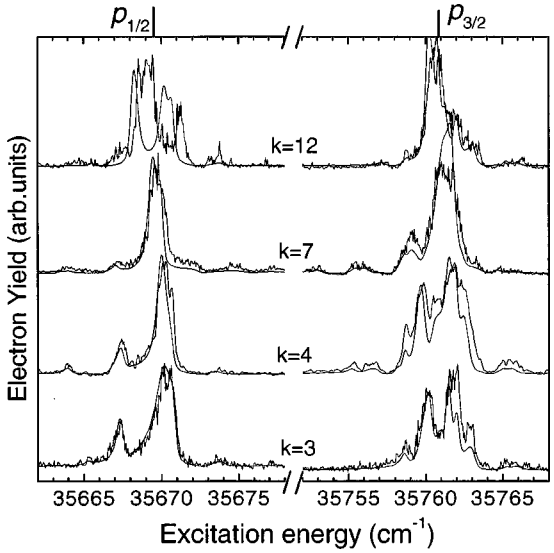

FIG. 5. An enlargment of the energy scale centered around the $3s\rightarrow 3p_{1/2}$ transition at 35 669.42 cm^{-1} and the $3s\rightarrow 3p_{3/2}$ transition at 35 760.97 cm^{-1} of the electron yield as a function of isolated-core excitation energy starting with the $3s16k$ Stark states with k = 3, 4, 7, and 12 as labeled in Fig. 2(b). The smooth lines are the theoretical calculations developed in part I [11].

100 cm^{-1} for an initial low-l state in field-free conditions as seen in Fig. 3(a). Upon introduction of a static electric field the angular momentum of the initial Rydberg electron is no longer conserved and the degenerate Rydberg state splits up into Stark states. Starting from a pure Stark state we observe a shake-up width of only 5 cm^{-1}. Thus we can view an electron in an initial Stark state even more as a spectator than an electron in an initial low-l state. The difference in the shake-up width is due to the additional angular oscillation of the Stark electron. It may recur radially every 0.6 ps; however, most of the time the Stark electron will be in high ($l>3$) angular momentum, describing a more circular orbit, far from the core region. The angular oscillation period at 1600 V/cm is about 10 ps. The initial $3s$ low-l states are slightly mixed with Stark character at 1600 V/cm and the shake-up width decreases from 100 cm^{-1} in zero-field to 50 cm^{-1} in 1600 V/cm.

The difference in the shakeup width can be understood in the angular-momentum picture: ICE of an initial Stark state only affects the low-angular-momentum fraction. The higher-angular-momentum fraction, with $l>3$, has a quantum defect of approximately zero before and after the ICE. In other words, most of the Stark state is not changed by the excitation of the core and the shakeup can only be small. The smallest shakeup possible would lead to only one peak per spin channel in the autoionization spectra. The notion that the dipole moment k of the Stark states hardly changes in an optical excitation has also been observed in far-infrared ionization of Rydberg-Stark atoms [14]. For an initial magnesium Stark state the change in dipole moment is small but not strictly zero. Note that there are only 13 initial Stark states $3snk$ and 16 final Stark states $3pn'k'$. At 1600 V/cm the 13 initial Stark states are spread over more or less the same energy region as the final 16 Stark states. Therefore the spacing between the initial states is larger (3.4 cm^{-1}) than for the final states (3.0 cm^{-1}). Upon the ICE the reddest initial Stark state $k=3$ [k is just a label here, see Fig. 2(a)] is projected onto (in hydrogenic labeling) the $k'=-13$ and $k'=-15$ states. The $k=4$ state is projected onto $k'=-13$ and $k'=-11$, and so on. This is well observed for the $P_{1/2}$ spin channel as shown in Fig. 5.

For the $P_{3/2}$ channel the autoionization spectra are more complicated. The differences between the $P_{1/2}$ and the $P_{3/2}$ channel as seen in Fig. 5 is caused by configuration interaction. The $k'=-15$ and $k'=-13$ of the $n=16$ manifold of the $P_{3/2}$ channel are interleaved with the $k'=-11$ and $k'=-9$ of the $n=18$ manifold of the $P_{1/2}$ channel. All these four states are localized on the same, down potential side of the atom in a field, making configuration interaction favorable. Also $P_{3/2}$ $n=14$ blue states are degenerate with the reddest $P_{1/2}$ $n=16$ states, but since the blue states are localized on the uphill side of the potential, no configuration interaction is observed for $P_{1/2}$. Configuration interaction makes it very hard to theoretically fit all details of Fig. 5. The $P_{1/2}$ channel gives a far better fit that the $P_{3/2}$ channel. The observed width in Fig. 5 of the final Stark states is 1 cm^{-1} corresponding to a lifetime of 15 ps. That indicates that the probability of the Stark states to autoionize upon core passage is high: the electron density has autoionized within about two angular recurrences.

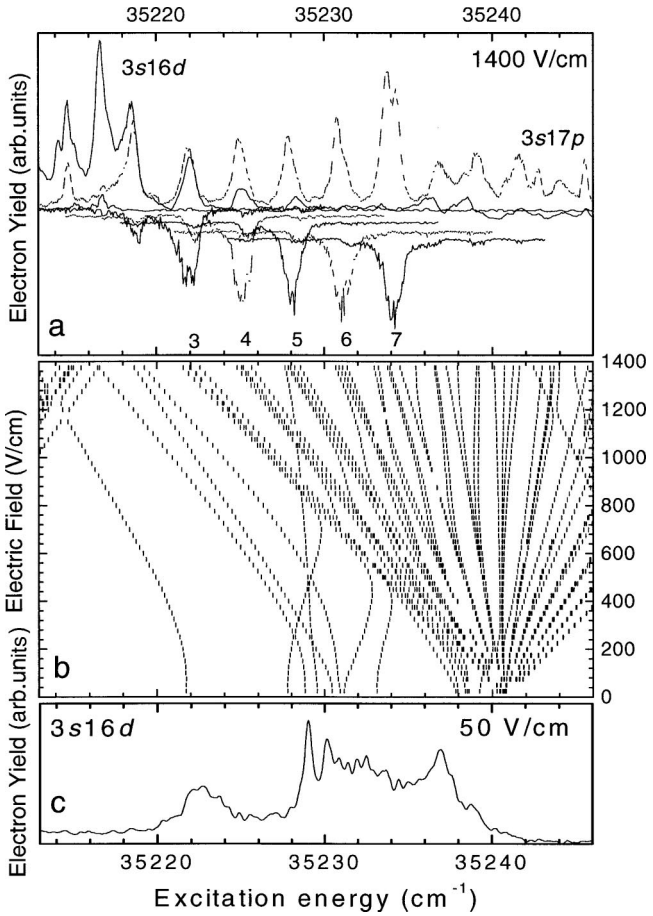

FIG. 6. (a) Electron yield as a function of isolated-core excitation energy minus the initial binding energy. Initial states are $3s16d$ (solid), $3s17p$ (dotted), and the five reddest Stark states (3–7; upside down). (b) Simulation of the energy of the $3p$ channel states as a function of electric field. (c) Electron yield as a function of isolated-core excitation energy minus the initial binding energy for an the initial states $3s16d$ at 50 V/cm.

As we have seen in part I [11], the only difference between the various initial states is their overlap integral with the $3p$ channels and their initial binding energy [Eq. (10) of [11]]. They autoionize essentially via the same $3p$ states. In Fig. 6(a) we plotted the ICE electron yield spectra of various initial states as a function of isolated-core excitation frequency minus the initial binding energy of the states in a field of 1400 V/cm. In other words, the ICE spectra are plotted as a function of energy above the $3s$ channel ionization limit. For clarity only a small energy region around the $P_{1/2}$ transition is shown. The solid line is the ICE spectrum starting from the $3s16d$ state, the dotted line starting from the $3s17p$ state. The ICE spectra starting from the reddest five Stark states are plotted upside down. It is clear the same $3p$ states are seen starting from different initial states. The only difference in the spectra is the overlap. In Fig. 6(b) a theoretical spectrum is shown of the energy of the $3p$ autoionizing states as a function of field strength [like Fig. 2(a) for the $3s$ states]. All m states are shown. In our experiment both

excitation lasers were parallel with the electric field and only $m=0$ states can be reached. For comparison, at low field the ICE spectrum starting from the $3s16d$ state in 50 V/cm is shown in Fig. 6(c). Starting from zero field the $n=16$ Stark manifold fans out around 35 241 cm^{-1}. In these low fields, however, only the states with d character can be reached and we observe broad features around 35 222 and 35 232 cm^{-1}. Upon increasing the field the d states are mixed into the Stark manifold and at 500 V/cm the Stark states have acquired enough d character to show up in the ICE spectra (compare Fig. 3). Finally, at 1600 V/cm all low-l states are mixed into the Stark manifold that we observe in Fig. 6(a).

VI. IMPLICATIONS FOR DIELECTRONIC RECOMBINATION

Let us divide the autoionization experiment into three parts: Excitation from the Mg ground state to the initial Rydberg states in the $3s$ channel, the radiative excitation (the ICE) to the $3p$ channel, and electron emission. Dielectronic recombination (DR) is the time inverse process: capture of a free electron by excitation of a Mg ion into a doubly excited neutral, radiative decay to a singly excited state and radiative decay to the Mg ground state. The second step of both processes involve the same couplings between states. What can we learn from an autoionization experiment that is important for DR?

The DR rate is proportional to $\Gamma_{a,\rho}\Gamma_{R,\rho}/(\Gamma_{a,\rho}+\Gamma_{R,\rho})$ (i.e., proportional to the rate of capture $\Gamma_{a,\rho}$ into the autoionizing states ρ times the branching ratio for photon emission $\Gamma_{R,\rho}$) [17]. Each autoionizing state ρ with a rate of capture $\Gamma_{a,\rho}$ larger than the photoemission rate $\Gamma_{R,\rho}$ contributes to DR. An electric field enhances DR [15] since it mixes the short-lived low-angular-momentum states with long-lived high-angular-momentum states. Effectively this increases the number of states that have a faster autoionization rate than the radiative rate. For the time-inverse process of DR, our autoionization measurement, the same rates are important. In the first excitation step we can choose which initial $3s$ state to probe, provided it has oscillator strength from the ground state. In the second step the strength of the coupling between the $3s$ and $3p$ channels leads to a shakeup width for autoionization or a radiative decay $\Gamma_{R,\rho}$ for DR. If electron emission (third step) of a populated state in the $3p$ channel is observed, it implies that its autoionization rate $\Gamma_{a,\rho}$ is larger than its radiative rate $\Gamma_{R,\rho}$ back to the $3s$ channel. In other words, what we detect is proportional to the radiative rate $\Gamma_{R,\rho}$ into the autoionizing states ρ times the branching ratio for autoionization $\Gamma_{a,\rho}$, so together $\Gamma_{R,\rho}\Gamma_{a,\rho}/(\Gamma_{a,\rho}+\Gamma_{R,\rho})$, where $\Gamma_{a,\rho}>\Gamma_{R,\rho}$. This is equal to the DR rate into the selected Rydberg state.

Measuring the autoionization yield of an initial $3s$ state is identical to detecting the partial DR cross section for that state. Integration of the autoionization yield of all initial $3s$ states results in the total DR cross section. The advantage of an autoionization measurement is that we gain information about both the initial and final states in the second step with high resolution (equal to the laser bandwidth). Knowledge of the coupling between initial and final states can be important to explain, e.g., the enhancement of the DR cross section, owing to an electric or magnetic field.

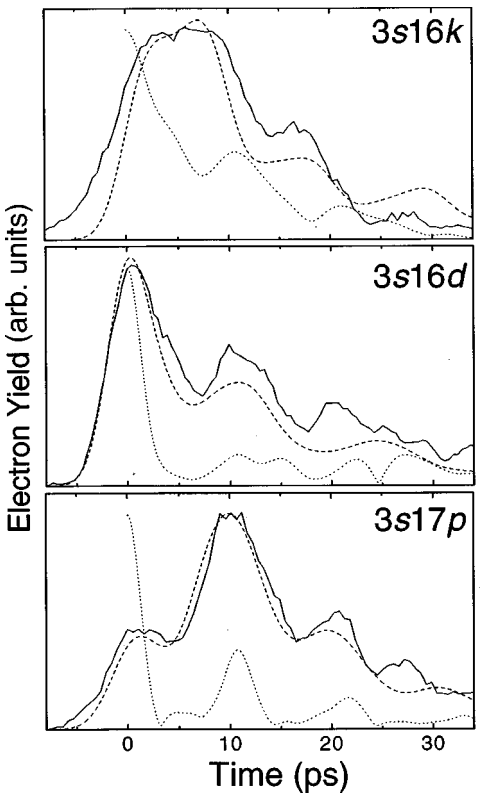

FIG. 7. The electron emission in time upon ICE starting from (a) the $3snk$, $k=4$ Stark state, (b) the $3s16d$ state, and (c) the $3s17p$ state in a field of 1400 V/cm. The solid line is the streak camera measurement, the dashed line is the calculation of the electron emission. For comparison the Fourier transform of the corresponding frequency spectrum multiplied by the bandwidth of the laser is also displayed (dotted line), corresponding to the electron density at the core.

VII. TIME-DEPENDENT ICE

In the above described experiment the isolated core was excited with a ns, narrow-band laser pulse. If the excitation is done with a short pulse, with a bandwidth larger than the spacing between the shake-up states, a coherent superposition of the final $3p$ states is created. Short pulse ICE is investigated in field-free conditions [4,9,10,12,13]. In a recent paper [7] we reported short pulse ICE in an electric field.

In Fig. 7 the initial states are a $3s16k$ Stark state with $k=4$ as labeled in Fig. 2(a), and the low-l states $3s16d$ and $3s17p$ in a field of 1400 V/cm. Shown is (solid lines) the electron emission as a function of time after sudden isolated core excitation with a laser pulse of 2 ps. The electron emission is detected with the atomic streak camera [22] with ps time resolution. The dashed lines are the simulations of the electron emission in time, based on the MQDT theory developed in part I [11]. Slight deviations can be attributed to the high excess kinetic energy ($\sim$4.3 eV) of the autoionized electrons. It is clear that the ICE spectra of Mg in an electric

field can be accurately simulated both in frequency and time.

The time-dependent behavior can be understood as follows. If the initial state is a Stark state, the sudden isolated core excitation will not affect the orbit much. Most of the Stark angular momentum is high and therefore its quantum defect is nearly zero. Only the low-angular-momentum part is suddenly changed, creating a ''shock-wave front'' [23]. This wave front starts oscillating over all angular momenta up to $l=n-1$ and back [24]. During this time there is a constant electron emission until the wave front returns to low angular momentum. At that time, when the shock wave front passes over the angular momenta it was originally created in, the electron emission suddenly drops to remain constant again for a second angular oscillation period. The result is a stepwise electron emission. A similar stepwise behavior of the electron emission is expected [13] when a Rydberg atom is exposed to a laser field that is *suddenly* turned on. The step time corresponds to the oscillation time of the Rydberg electron and the step height is the probability of autoionization upon core passage of the Rydberg electron. In Fig. 7(a) we observe that the oscillation time of the $3s16k$ Stark state is 10 ps in 1400 V/cm and the probability of autoionizing after ICE is about 60%.

The electron emission is entirely different if we start with an initial, stationary, low-l state [Figs. 7(b) and 7(c)]. Upon sudden ICE the electronic wave function is projected on a coherent superposition of final $3p$ states that are affected by the electric field. The result is an oscillation in angular momentum, starting at the particular low l. Each time, after an angular oscillation period, it recurs to the core and has a probability to autoionize. The detected electron emission therefore shows an oscillatory behavior. The period of oscillation, again, corresponds to the orbital time of the electron in 1400 V/cm.

The electron emission is the flux of electron density that escapes over the saddle point. We would like to compare this flux with the electron density at the core. Fourier transforming the frequency spectra provides us with that information. The detected frequency spectra from Fig. 4 are multiplied by a Gaussian with a bandwidth of 7 cm^{-1} (corresponding to the 2-ps pulse) and Fourier transformed. The resulting curves (dotted lines in Fig. 7) give the recurrence probability of the initial excitation conditions [25]. For an initial low-l state this means the recurrence to that low l in the vicinity of the ionic core. At $t=0$ the probability is normalized, whereafter the probability shows a periodic, oscillatory behavior. At the moment of recurrence there is a probability of electron emission. As one can indeed see, the periodicity in Figs. 7(b) and 7(c) for electron emission and recurrence are identical. The intensity is not necessarily the same. For example, the electron density at the core right after sudden ICE of an initial $3s17p$ state is high [Fig. 7(c)]. This does not, however, result in strong electron emission. Most emission occurs at the first electron recurrence to the core after one angular oscillation.

For an initial Stark state the electron emission after sudden ICE and the Fourier-transformed ICE frequency spectrum are distinctly different [Fig. 7(a)]: Fourier transforming the frequency spectrum actually provides us with the recurrence of the shock wave front rather than the electron density at the core. At the moment of sudden ICE the shock wave starts close to the core. Simultaneously the constant electron emission begins. After one angular oscillation period (10 ps) the shock wave returns to the core and suddenly the electron emission drops. This happens a second time at 21 ps.

VIII. CONCLUSIONS

We performed isolated-core excitation of magnesium atoms in an electric field and monitored the autoionization yield as a function of isolated-core excitation frequency. We started with different initial states in various electric fields. The various initial states around $n=16$ lead to very different shakeup widths upon ICE: An initial low-l state has a much larger shakeup width (100–50 cm^{-1}) than an initial Stark state (5 cm^{-1}). All spectra can be accurately fitted with the MQDT theory that is developed in part I, for all fields, both in frequency and time. Comparing the autoionization measurements with dielectronic recombination measurements, we find that these measurements are in essence the same. Detecting autoionization, however, has the advantage that it is much easier and it displays a high resolution to discern the states that are involved. Finally, we compared the Fourier transform of the frequency spectra with time-dependent electron emission measurements of ICE. For initial low-l states the same periodic behavior is observed; for an initial Stark state, however, the electron emission is stepwise and the FT of the frequency spectrum provides us with the recurrence spectrum of the excitation shock wave. If the shock wave returns to the core, the electron emission suddenly drops.

ACKNOWLEDGMENTS

It is a pleasure to thank C. Wesdorp for assistance in the experiments concerning the time domain. The work described in this paper is part of the research program of the FOM (Foundation for Fundamental Research on Matter) and was made possible by the financial support from NWO (Netherlands Organization for the Advancement of Research). F.R. was supported by the NFS.

[1] W. E. Cooke, T. F. Gallagher, S. A. Edelstein, and R. M. Hill, Phys. Rev. Lett. **41**, 178 (1978).

[2] T. F. Gallagher, *Rydberg Atoms* (Cambridge University Press, Cambridge, 1994).

[3] C. J. Dai, G. W. Schinn, and T. F. Gallagher, Phys. Rev. A **42**, 223 (1990); G. W. Schinn, C. J. Dai, and T. F. Gallagher, *ibid.* **43**, 2316 (1991).

[4] J. G. Story, D. I. Duncan, and T. F. Gallagher, Phys. Rev. Lett. **71**, 3431 (1993).

[5] M. D. Lindsey, C. J. Dai, B. J. Lyons, C. R. Mohon, and T. F. Gallagher, Phys. Rev. A **50**, 5058 (1994).

[6] N. J. van Druten and H. G. Muller, J. Phys. B **29**, 15 (1996).

[7] J. B. M. Warntjes, C. Wesdorp, F. Robicheaux, and L. D. Noordam, Phys. Rev. Lett. **83**, 512 (1999).
[8] L. D. Noordam, H. Stapelfeldt, D. I. Duncan, and T. F. Gallager, Phys. Rev. Lett. **68**, 1496 (1992).
[9] B. J. Lyons, D. W. Schumacher, D. I. Duncan, R. R. Jones, and T. F. Gallager, Phys. Rev. A **57**, 3712 (1998).
[10] R. R. Jones, Phys. Rev. A **57**, 446 (1998).
[11] F. Robicheaux, preceding paper Phys. Rev. A **61**, 033406 (2000).
[12] J. E. Thoma and R. R. Jones, Phys. Rev. Lett. **83**, 516 (1999).
[13] J. H. Hoogenraad and L.D. Noordam, in *Super-Intense Laser-Atom Physics*, edited by B. Pireaux (Plenum Press, New York, 1993), p. 269.
[14] G. M. Lankhuijzen, M. Drabbels, F. Robicheaux, and L. D. Noordam, Phys. Rev. A **57**, 440 (1998).
[15] V. L. Jacobs, J. Davis, and P. C. Kepple, Phys. Rev. Lett. **37**, 1390 (1976); V. L. Jacobs and J. Davis, Phys. Rev. A **19**, 776 (1979).
[16] A. Müller *et al.*, Phys. Rev. Lett. **56**, 127 (1986).
[17] F. Robicheaux and M. S. Pindzola, Phys. Rev. Lett. **79**, 2237 (1997); T. Bartsch *et al.*, *ibid.* **79**, 2233 (1997).
[18] L. Ko, V. Klimenko, and T. F. Gallagher, Phys. Rev. A **59**, 2126 (1999).
[19] C. E. Moore, *Atomic Energy Levels*, Natl. Bur. Stand. (U.S.) Circ. No. 467 (1949).
[20] L. D. Noordam, M. P. de Boer, and H. B. van Linden van den Heuvel, Phys. Rev. A **41**, 6267 (1990).
[21] A. ten Wolde, L. D. Noordam, H. G. Muller, A. Lagendijk, and H. B. van Linden van den Heuvel, Phys. Rev. Lett. **61**, 2099 (1988).
[22] G. M. Lankhuijzen and L. D. Noordam, Opt. Commun. **129**, 361 (1996); Phys. Rev. Lett. **76**, 1784 (1996).
[23] X. Wang and W. E. Cooke, Phys. Rev. Lett. **67**, 976 (1991); Phys. Rev. A **46**, 4347 (1992); **46**, R2201 (1992).
[24] L. D. Noordam, A. ten Wolde, A. Lagendijk, and H. B. van Linden van den Heuvel, Phys. Rev. A **40**, 6999 (1989).
[25] G. M. Lankhuijzen and L. D. Noordam, Phys. Rev. A **52**, 2016 (1995); Phys. Rev. Lett. **76**, 1784 (1996).